A Novel Estimation Methodology for Tracheal Pressure in Mechanical Ventilation Control

Milos Ajcevic, Andrea De Lorenzo, Agostino Accardo, Alberto Bartoli and Eric Medvet
DIA - University of Trieste Trieste, Italy
Email: milos.ajcevic@phd.units.it, andrea.delorenzo@phd.units.it, accardo@units.it, bartoli.alberto@units.it and emedvet@units.it

***Abstract*—High-frequency percussive ventilation (HFPV) is a non-conventional mechanical ventilatory strategy which has proven useful in the treatment of a number of pathological conditions. HFPV usually involves the usage of endotracheal tubes (EET) connecting the ventilator circuit to the airway of the patient. The pressure of the air flow insufflated by HFPV must be controlled very accurately in order to avoid barotrauma and volutrauma. Since the actual tracheal pressure cannot be measured, a model for estimating such a pressure based on the EET properties and on the air flow properties that can actually be measured in clinical practice is necessary. In this work we propose a novel methodology, based on Genetic Programming, for synthesizing such a model. We experimentally evaluated our models against the state-of-the-art baseline models, crafted by human experts, and found that our models for estimating tracheal pressure are significantly more accurate.**

I. Introduction

High-frequency percussive ventilation (HFPV) is a non-conventional ventilatory strategy which associates the beneficial aspects of conventional mechanical ventilation (CMV) with those of high-frequency ventilation HFV [1]. HFPV acts as a rhythmic cyclic ventilation with physically servoed flow regulation, which produces a controlled staking tidal volume by pulsatile flow [1], [2]. Over the years, HFPV has proven highly useful in the treatment of several widely differing pathological conditions: closed head injury [3], patients with acute respiratory distress syndrome (ARDS) caused by burns and smoke inhalation [4], [5], newborns with hyaline membrane disease and/or ARDS [6], patients with severe gas exchange impairment [7]. The efficacy of HFPV has been demonstrated also in removing bronchial secretions under diverse conditions [8], [9].

Usage of HFPV in clinical practice involves endotracheal tubes (EET) for connecting the ventilator circuit to the airway of the patient. The pressure measured by the ventilator consists of the sum of the EET pressure drop and of the tracheal pressure dissipated to inflate lung. In order to evaluate correctly the respiratory function, in particular, to avoid barotrauma and volutrauma [10], it is mandatory to take into account precisely the real amount of pressure dissipated by these components [11], [12]. While the pressure at the ventilator end of the EET can be measured easily, measuring the tracheal pressure of a patient is more difficult and, in every day clinical practice, such a measure cannot be done invasively. For this reason, HFPV requires a model for accurately estimating the tracheal pressure value based solely on non-invasive pressure and flow measurements.

In this paper, we describe the synthesis of such model by means of Genetic Programming (GP). GP is a method for automatically generating solutions—in the form of computer programs, formulas, and so on—inspired by biological evolution. We experimentally evaluated our approach by comparing our GP-generated model against two different models largely used in previous works [13], [14] on a dataset of in vitro measures. The outcomes are very important: the GP-generated models exhibit an estimation accuracy which is sensibly higher than those of the existing models which has been crafted by human experts and have been largely used in previous works.

II. Related work

The pressure drop during mechanical ventilation $\Delta P_{\text{EET}}(t) = P_{\text{aw}}(t) – P_{\text{tr}}(t)$—where $P_{\text{aw}}(t)$ is the airway pressure measured by ventilator and $P_{\text{tr}}(t)$ is the unknown tracheal pressure—has been widely studied both in adult and pediatric endotracheal tubes [10]–[19]. In general, ΔP_{EET} depends on flow regime, on geometric characteristics of the tube and on physical properties of the gas. The flow regime can be either laminar or turbulent with a small transitional region between these two regimes. In order to estimate ΔP_{EET} and derive tracheal pressure accordingly, a model for the pressure-flow relationship characterizing EET is necessary. This model may be considered linear in the presence of laminar flow [15], [16]:

$$\Delta P_{\text{EET}}(t) = R_{\text{tube}}\dot{V}(t) \tag{1}$$

where $\dot{V}(t)$ is the flow and R_{tube} is the flow resistance coefficient. In most cases, though, a nonlinear pressure-flow model turns out to be more appropriate due to the presence of turbulent flow [10], [14], [17]–[19]:

$$\Delta P_{\text{EET}}(t) = K_1\dot{V}(t) + K_2\dot{V}(t)|\dot{V}(t)| \tag{2}$$

where and K_1 and K_2 are the Rohrer's constants [20].

The above approaches may not be sufficiently accurate during high frequency oscillatory ventilation. Further models have been developed for such scenarios by taking into account an additional pressure drop $\Delta P_I(t)$ due to mechanical inertance I and depending on the volume acceleration $\ddot{V}(t)$ [13], [14]:

$$\Delta P_{\text{I}}(t) = I\ddot{V}(t) \tag{3}$$

III. Our approach

Our approach is based on Genetic Programming (GP). GP is an automatic method for creating computer programs inspired by biological evolution [21]. GP has been used in a wide

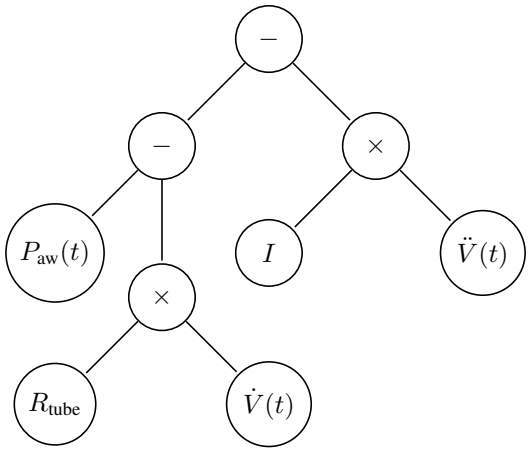

Figure 1. Tree representation of the "$P_{\text{aw}}(t) - R_{\text{tube}}\dot{V}(t) - I\ddot{V}(t)$" formula.

range of applications such as web security [22], electricity price prediction [23], text mining [24]. In GP, a *population* of computer programs is generated at random starting from a predefined set of building blocks. Each of these programs constitutes a candidate solution for the problem and is called an *individual*. The process is based on a predefined *fitness function* for the problem to be solved. This function quantifies the performance of any given candidate solution for that problem. Usually, the fitness of an individual is computed on a set of solved instances of the problem (the *learning corpus*) by comparing—in terms of some predefined performance index—the solutions provided by the individual against the known correct solutions.

A GP execution consists in an evolutionary search structured as follows: (i) compute the fitness of each individual; (ii) construct new individuals by applying certain *genetic operators* (such as "crossover" and "mutation") to the individuals with highest fitness; (iii) construct a new population composed of individuals with highest fitness and new individuals as created at the previous step. These steps constitute a *generation*. This process is iterated until either a solution with perfect fitness is found or some termination criterion is satisfied, e.g., a predefined maximum number of generations have evolved. Usually, the population size is kept constant across all generations.

In many scenarios of practical interest, each GP individual represents a formula rather than a more general computer program. The formula is represented as an abstract syntax tree, where a branch node is an element taken from a predefined *functions set* and a leaf node is an element taken from a predefined *terminal set* (terminal set and function set constitute the building blocks mentioned above). The *function set* may contain mathematical functions like the arithmetic operators whereas the *terminal set* usually contains constants and variables. An example of a GP tree individual which corresponds to a formula is showed in Figure 1.

In this work, we aim at estimating the tracheal pressure $P_{\text{tr}}(t)$. To this end, we use a terminal set which consists of:

- the pressure measured by ventilator $P_{\text{aw}}(t)$,
- the flow $\dot{V}(t)$,
- the volume acceleration $\ddot{V}$(t),

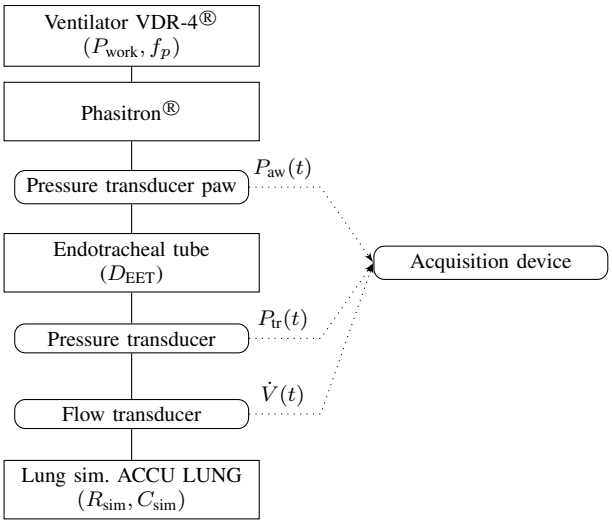

Figure 2. Diagram of the experimental setup: measurement equipment is denoted by blocks with rounded corners. Equipment parameters are shown inside corresponding blocks.

- the percussive frequency f_p,
- the work pressure P_{work},
- random constants uniformly distributed in $[0.01, 10]$.

Note that we do not include the parameters of the lung simulator (R_{sim} and C_{sim}, see Section IV-A) because their values are hardly estimable with precision during the clinical practice.

The function set is composed by the mathematical binary operators $+$, $-$, $\times$, $\div$, $\exp$ and the exponentiation pow.

We used two fitness function to be minimized: (i) the Mean Square Error (MSE) and (ii) the individual size, i.e., the total number of nodes of the individual in its tree form:

$$f_{\text{MSE}}(T) = \frac{1}{n}\sum_{i=1}^{n}(\hat{P}_T(t_n) - P_{\text{tr}}(t_n))^2 \quad (4)$$

$$f_{\mathcal{S}}(T) = \mathcal{S}(T) \quad (5)$$

where T indicates a GP individual, $\hat{P}_T(t_n)$ is the value assumed by the individual T at time t_n and $\mathcal{S}(T)$ is the number of nodes in the individual T.

The choice to minimize the number of nodes is important in order to enforce a principle of parsimony, i.e., to reduce the possible proliferation of unnecessary sub-trees in individuals (also known as *bloat* [25]). We minimize the resulting *multi-objective* fitness by means of NSGA-II [26]. We performed our GP searches using a tool that we have developed in our lab [22]–[24]. This tool is written in Java and can run different GP searches in parallel on different machines.

IV. Experiments

A. Experimental setup

Figure 2 shows the experimental setup to collect in vitro measures for this study. HFPV was provided by a volumetric

diffusive respirator (VDR-4®[1]) which delivers mini-bursts of respiratory gas mixtures in the proximal airways by the Phasitron®, which is the heart of this kind of ventilation [1], [27]. In this experimental setup, pulsatile flow was delivered during inspiratory phase (In) while expiratory phase (Ex) was completely passive. The VDR-4® ventilator was set to deliver a inspiratory/expiratory (In/Ex) duration ratio of 1:1, both for the pulse and the overall respiratory cycle [1], [27].

The examined EET was connected[2] to the ventilator circuit and to a single-compartment lung simulator (ACCU LUNG)[3] that provides a physical model of the respiratory system.

Flow and pressures were acquired by a dedicated acquisition system [28]. The measurement of the flow signal $\dot{V}(t)$ was performed using Fleisch pneumotachograph[4] connected to a differential pressure transducer (0.25 INCH-D-4V[5]). The pressure signals $P_{\text{aw}}(t)$ and $P_{\text{tr}}(t)$ were measured with pressure transducers (ASCX01DN[6]) placed respectively before the EET connector and at the end of the EET, respectively. $\dot{V}(t)$, $P_{\text{aw}}(t)$ and $P_{\text{tr}}(t)$ signals were acquired at a sampling frequency of $f_s = 2000\,\text{Hz}$ with 12 bit resolution (PCI-6023E[7]). The volume acceleration $\ddot{V}(t)$ has been computed off-line as:

$$\ddot{V}(t_n) = \frac{\dot{V}(t_{n+1}) - \dot{V}(t_{n-1})}{2T_s} \tag{6}$$

where $T_s = \frac{1}{f_s} = 0.5\,\text{ms}$ and $\dot{V}(t_n)$ is the n-th measured sample of $\dot{V}(t)$.

We experimented with two different EET[8] with inner diameter of $D_{\text{EET}} = 6.5\,\text{mm}$ and $D_{\text{EET}} = 7.5\,\text{mm}$. For each EET, we considered all the 108 combinations of the following parameters:

- ventilator work pressure P_{work}, from $20\,\text{cm}_{\text{H}_2\text{O}}$ to $45\,\text{cm}_{\text{H}_2\text{O}}$ with increasing steps of $5\,\text{cm}_{\text{H}_2\text{O}}$;
- ventilator percussive frequency f_p, set to 300 cycle/min, 500 cycle/min and 700 cycle/min;
- lung simulator resistive load R_{sim}, set to $5\,\text{cm}_{\text{H}_2\text{O}}/(\text{L s})$ and $20\,\text{cm}_{\text{H}_2\text{O}}/(\text{L s})$;
- lung simulator compliance load C_{sim}, set to $10\,\text{mL/cm}_{\text{H}_2\text{O}}$, $20\,\text{mL/cm}_{\text{H}_2\text{O}}$ and $50\,\text{mL/cm}_{\text{H}_2\text{O}}$.

In each experiment we collected the values for $\dot{V}(t)$, $P_{\text{aw}}(t)$, $P_{\text{tr}}(t)$ and $\ddot{V}(t)$ during a single inspiratory phase of a single respiratory cycle, for a duration of 4 s. Hence, for each EET and for each parameter combination, we collected a *respiratory signals set* composed of 8000×4 samples. Figure 3 plots $P_{\text{tr}}(t)$ and $P_{\text{aw}}(t)$ of a single respiratory signal set, i.e., only two of the four components of that signal set. Table I summarizes the symbols used in this work.

B. Methodology

In order to generate a model for the unknown tracheal pressure $P_{\text{tr}}(t)$ for a given EET, we proceeded as follows.

[1]Percussionaire Corporation, USA.
[2]With a dedicated EET connector with inner diameter of 11 mm.
[3]Fluke Biomedical, USA.
[4]Type 2, Switzerland.
[5]All Sensors, USA.
[6]Honeywell, USA, with identical connectors with diameter of 20 mm.
[7]National Instruments, USA.
[8]I.D. 6.5, Rusch, Gremany and I.D. 7.5, Rusch, Gremany.

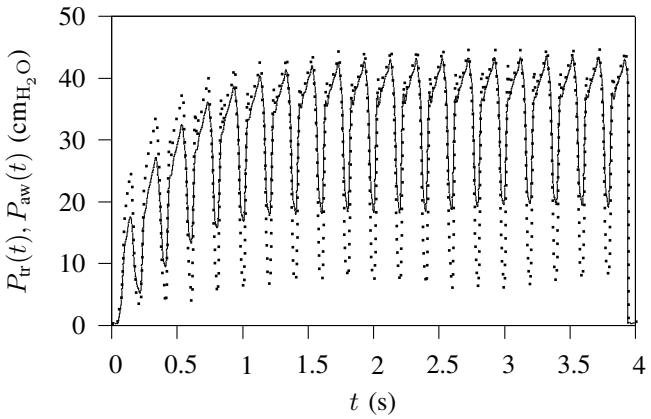

Figure 3. Measurements $P_{\text{tr}}(t)$ and $P_{\text{aw}}(t)$ for the EET with $D_{\text{EET}} = 6.5\,\text{mm}$ and the parameters combination $R_{\text{sim}} = 20\,\text{cm}_{\text{H}_2\text{O}}/(\text{L s})$, $C_{\text{sim}} = 10\,\text{mL/cm}_{\text{H}_2\text{O}}$, $f_p = 300\,\text{cycle/min}$ and $P_{\text{work}} = 40\,\text{cm}_{\text{H}_2\text{O}}$.

Table I. SUMMARY OF NOTATION

Symbol	Type	Description	Unit
D_{EET}	parameter	EET diameter	mm
R_{sim}	parameter	lung sim. resistive load	$\text{cm}_{\text{H}_2\text{O}}/(\text{L s})$
C_{sim}	parameter	lung sim. compliance load	$\text{mL/cm}_{\text{H}_2\text{O}}$
f_p	parameter	HFPV percussive frequency	cycle/min
P_{work}	parameter	HFPV work pressure	$\text{cm}_{\text{H}_2\text{O}}$
$P_{\text{aw}}(t)$	sampled signal	ventilator pressure	$\text{cm}_{\text{H}_2\text{O}}$
$P_{\text{tr}}(t)$	sampled signal	tracheal pressure	$\text{cm}_{\text{H}_2\text{O}}$
$\dot{V}(t)$	sampled signal	flow	L/s
$\ddot{V}(t)$	computed signal	volume acceleration	L/s^2

1) We randomly selected 7 respiratory signals sets and used them as training set. We randomly selected 3 other respiratory signals sets and used them as validation set. We used the remaining respiratory signal sets as testing set.
2) We executed a GP search as follows: (i) we ran 32 different and independent GP evolutions (*jobs*), each on the training set (without the examples in the validation set) and with the GP-related parameters set as in Table II; (ii) for each job and for each generation, we selected the individual with the best multi-objective fitness (according to NSGA-II) on the training set; (iii) among the resulting set of $32 \times 500 = 16000$ individuals, we selected the individual T^* with the lowest f_{MSE} on the validation set; (iv) we used the formula $\hat{P}_{T^*}(t)$ represented by T^* as a model for $P_{\text{tr}}(t)$.
3) We repeated steps 1 and 2 five times.

In other words, for each EET, we constructed five models for $P_{\text{tr}}(t)$ using five different learning sets.

Each GP search has been executed in parallel on 4 identical machines powered with a quad-core Intel Xeon X3323 (2.53 GHz) and 2GB of RAM.

In order to assess our results, we considered two baseline models widely used in the literature and crafted by human experts [13], [14]. The models are defined in accordance with Eq. 1 and Eq. 2 and with the addition of the volume

Table II. GP PARAMETERS

Parameter	Settings
Population size	500
Number of generations	500
Selection	Tournament of size 7
Initialization depths	1–5
Max. depth after crossover	15
Reproduction rate	10%
Crossover rate	80%
Mutation rate	10%

Table III. EXPERIMENT RESULTS

D_{EET}	Repetitions (MSE %)			Average (MSE %)			Time
	GP	LM	NM	GP	LM	NM	(min)
6.5	1.01	3.44	1.94	0.84	3.45	1.96	263
	0.78	3.47	1.92				
	0.76	3.57	1.98				
	0.82	3.48	1.89				
	0.84	3.29	2.06				
7.5	0.90	3.33	1.94	1.44	3.29	1.91	257
	1.06	3.35	1.95				
	1.03	3.24	1.90				
	3.21	3.27	1.89				
	1.03	3.25	1.94				

acceleration $\ddot{V}(t)$ (Eq. 3), as follows:

$$\text{LM: } P_{\text{tr}}(t) = P_{\text{aw}}(t) - R_{\text{tube}}\dot{V}(t) - I\ddot{V}(t)$$
$$\text{NM: } P_{\text{tr}}(t) = P_{\text{aw}}(t) - K_1\dot{V}(t) - K_2\dot{V}(t)|\dot{V}(t)| - I\ddot{V}(t)$$

We selected the parameter values for these baseline models by means of Least Squares method applied on the same learning data available to each GP search. That is, we used a different parameter calibration for each GP search, based on the union of the training and validation sets randomly selected for that search.

The accuracy of the GP-generated models and the baseline models LM and NM was quantified by the respective mean square error MSE exhibited on the testing set.

C. Results

The salient results are summarized in Table III. The execution time indicates the average time required for generating one of the GP-based models.

The key result is that the GP-generated model performs significantly better than the baseline in all the experiments, with the only exception of the fourth repetition for $D_{\text{EET}} = 7.5\,\text{mm}$ in which the GP-generated model performs slightly better than LM but worse than NM.

In order to gain further insights into the ability of GP to generate accurate models, we report in Figure 4 the cumulative distribution of the MSE on the testing set of all the best individuals selected on the validation set—i.e., at the end of each job. The baseline models are reported as vertical lines. It can be seen that the good performances exhibited by our approach are not caused by a single lucky individual: GP is instead able to systematically produce a large set of models which perform better than the baseline models.

Figure 5 plots, for each of the $5 \times 32 = 160$ best individuals found at the end of each job and each repetition, the MSE on the validation vs. the MSE on the testing set. The figure shows how the performance of an individual on the validation set is a good predictor of the performance on the testing set, which hence suggests that the proposed method could be applied successfully also for different EET and parameter combinations.

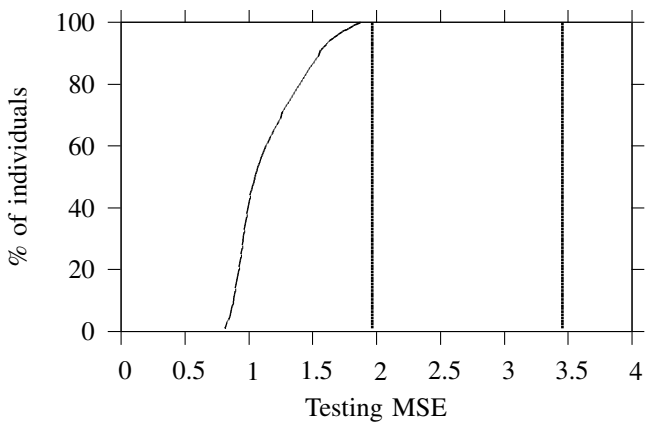

(a) $D_{\text{EET}} = 6.5\,\text{mm}$

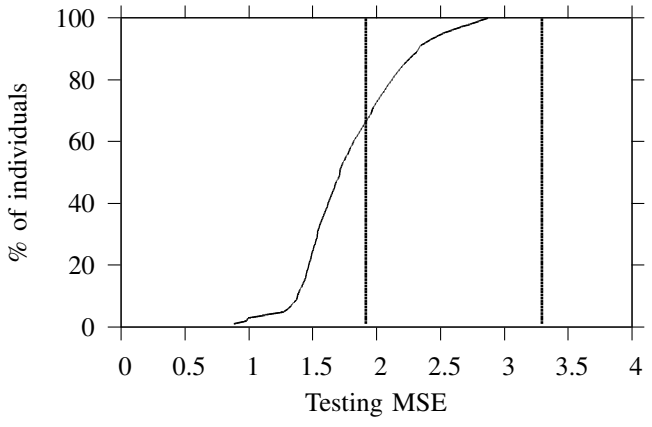

(b) $D_{\text{EET}} = 7.5\,\text{mm}$

Figure 4. Cumulative distribution of the MSE on the testing set for the final individual of each job. Vertical lines indicate the MSE for the two baseline models NM and LM.

V. CONCLUDING REMARKS

We proposed a novel approach for estimating the tracheal pressure during High-frequency percussive ventilation (HFPV), a problem of uttermost importance in clinical pratice. Our approach is based on genetic programming (GP) which synthesizes a model for the tracheal pressure automatically, based on a collection of respiratory signals.

We assessed our proposal on a dataset consisting of in vitro measured respiratory signals. The results in terms of Mean Square Error are very good: the GP-generated models for the tracheal pressure perform significantly better than two other existing models—generated by human experts—largely used in earlier proposals.

REFERENCES

[1] U. Lucangelo, V. Antonaglia, W. Zin, L. Fontanesi, A. Peratoner, F. Bird, and A. Gullo, "Effects of mechanical load on flow, volume and pressure delivered by high-frequency percussive ventilation," *Respiratory physiology & neurobiology*, vol. 142, no. 1, pp. 81–91, 2004.

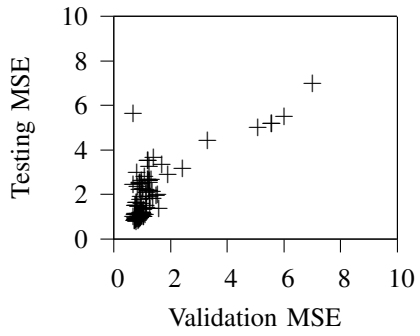

(a) $D_{\mathrm{EET}} = 6.5\,\mathrm{mm}$

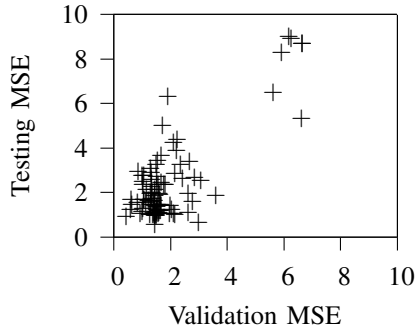

(b) $D_{\mathrm{EET}} = 7.5\,\mathrm{mm}$

Figure 5. Validation MSE vs. testing MSE: each cross corresponds to an individual.

[2] U. Lucangelo, A. Accardo, A. Bernardi, M. Ferluga, M. Borelli, V. Antonaglia, F. Riscica, and W. A. Zin, "Gas distribution in a two-compartment model ventilated in high-frequency percussive and pressure-controlled modes," *Intensive care medicine*, vol. 36, no. 12, pp. 2125–2131, 2010.

[3] J. M. HURST, R. D. BRANSON, and C. B. DEHAVEN, "The role of high-frequency ventilation in post-traumatic respiratory insufficiency," *The Journal of Trauma and Acute Care Surgery*, vol. 27, no. 3, pp. 236–242, 1987.

[4] C. W. Lentz and H. Peterson, "Smoke inhalation is a multilevel insult to the pulmonary system," *Current Opinion in Pulmonary Medicine*, vol. 3, no. 3, pp. 221–226, 1997.

[5] S. K. Alpard, J. B. Zwischenberger, W. Tao, D. J. Deyo, D. L. Traber, and A. Bidani, "New clinically relevant sheep model of severe respiratory failure secondary to combined smoke inhalation/cutaneous flame burn injury," *Critical care medicine*, vol. 28, no. 5, pp. 1469–1476, 2000.

[6] G. C. Velmahos, L. S. Chan, R. Tatevossian, E. E. Cornwell, W. R. Dougherty, J. Escudero, and D. Demetriades, "High-frequency percussive ventilation improves oxygenation in patients with ards," *CHEST Journal*, vol. 116, no. 2, pp. 440–446, 1999.

[7] S. M. Paulsen, G. W. Killyon, D. J. Barillo, M. A. CROCE, and S. PAULSEN, "High-frequency percussive ventilation as a salvage modality in adult respiratory distress syndrome: A preliminary study. discussion," *The American surgeon*, vol. 68, no. 10, pp. 852–856, 2002.

[8] K. Deakins and R. L. Chatburn, "A comparison of intrapulmonary percussive ventilation and conventional chest physiotherapy for the treatment of atelectasis in the pediatric patient," *Respiratory care*, vol. 47, no. 10, pp. 1162–1167, 2002.

[9] U. Lucangelo, V. Antonaglia, W. A. Zin, M. Confalonieri, M. Borelli, M. Columban, S. Cassio, I. Batticci, M. Ferluga, M. Cortale *et al.*, "High-frequency percussive ventilation improves perioperatively clinical evolution in pulmonary resection*," *Critical care medicine*, vol. 37, no. 5, pp. 1663–1669, 2009.

[10] P. Rocco and W. Zin, "Modelling the mechanical effects of tracheal tubes in normal subjects," *European Respiratory Journal*, vol. 8, no. 1, pp. 121–126, 1995.

[11] A. D. Bersten, A. J. Rutten, A. E. Vedig, G. A. Skowronski *et al.*, "Additional work of breathing imposed by endotracheal tubes, breathing circuits, and intensive care ventilators." *Critical care medicine*, vol. 17, no. 7, p. 671, 1989.

[12] P. Bolder, T. Healy, A. Bolder, P. Beatty, and B. Kay, "The extra work of breathing through adult endotracheal tubes," *Anesthesia & Analgesia*, vol. 65, no. 8, pp. 853–859, 1986.

[13] S. Schumann, M. Krappitz, K. Möller, R. Hentschel, G. Braun, and J. Guttmann, "Pressure loss caused by pediatric endotracheal tubes during high-frequency-oscillation-ventilation," *Respiratory physiology & neurobiology*, vol. 162, no. 2, pp. 132–137, 2008.

[14] M. Sullivan, J. Paliotta, and M. Saklad, "Endotracheal tube as a factor in measurement of respiratory mechanics," *Journal of applied physiology*, vol. 41, no. 4, pp. 590–592, 1976.

[15] W. Zin, L. Pengelly, and J. Milic-Emili, "Active impedance of respiratory system in anesthetized cats," *Journal of Applied Physiology*, vol. 53, no. 1, pp. 149–157, 1982.

[16] G. Conti, R. De Blasi, A. Lappa, A. Ferretti, M. Antonelli, M. Bufi, and A. Gasparetto, "Evaluation of respiratory system resistance in mechanically ventilated patients: the role of the endotracheal tube," *Intensive care medicine*, vol. 20, no. 6, pp. 421–424, 1994.

[17] P. Behrakis, B. Higgs, A. Baydur, W. Zin, and J. Milic-Emili, "Respiratory mechanics during halothane anesthesia and anesthesia-paralysis in humans," *Journal of Applied Physiology*, vol. 55, no. 4, pp. 1085–1092, 1983.

[18] D. J. Prezant, T. K. Aldrich, J. P. Karpel, and S. S. Park, "Inspiratory flow dynamics during mechanical ventilation in patients with respiratory failure," *American Journal of Respiratory and Critical Care Medicine*, vol. 142, no. 6 Pt 1, pp. 1284–1287, 1990.

[19] A. Lorino, L. Beydon, C. Mariette, E. Dahan, and H. Lorino, "A new correction technique for measuring respiratory impedance through an endotracheal tube," *European Respiratory Journal*, vol. 9, no. 5, pp. 1079–1086, 1996.

[20] F. Rohrer, "Der strömungswiderstand in den menschlichen atemwegen und der einfluss der unregelmässigen verzweigung des bronchialsystems auf den atmungsverlauf in verschiedenen lungenbezirken," *Pflügers Archiv European Journal of Physiology*, vol. 162, no. 5, pp. 225–299, 1915.

[21] J. R. Koza, "Genetic Programming: On the Programming of Computers by Means of Natural Selection (Complex Adaptive Systems)," 1992.

[22] E. Medvet, C. Fillon, and A. Bartoli, "Detection of web defacements by means of genetic programming," in *Information Assurance and Security, 2007. IAS 2007. Third International Symposium on*. IEEE, 2007, pp. 227–234.

[23] A. Bartoli, G. Davanzo, A. De Lorenzo, and E. Medvet, "Gp-based electricity price forecasting," in *Genetic Programming*, ser. Lecture Notes in Computer Science, S. Silva, J. Foster, M. Nicolau, P. Machado, and M. Giacobini, Eds. Springer Berlin Heidelberg, 2011, vol. 6621, pp. 37–48. [Online]. Available: http://dx.doi.org/10.1007/978-3-642-20407-4_4

[24] A. Bartoli, G. Davanzo, A. De Lorenzo, M. Mauri, E. Medvet, and E. Sorio, "Automatic generation of regular expressions from examples with genetic programming," in *Proceedings of the fourteenth international conference on Genetic and evolutionary computation conference companion*. ACM, 2012, pp. 1477–1478.

[25] P. A. Whigham and G. Dick, "Implicitly controlling bloat in genetic programming," *Evolutionary Computation, IEEE Transactions on*, vol. 14, no. 2, pp. 173–190, 2010.

[26] K. Deb, A. Pratap, S. Agarwal, and T. Meyarivan, "A fast and elitist multiobjective genetic algorithm: Nsga-ii," *Evolutionary Computation, IEEE Transactions on*, vol. 6, no. 2, pp. 182 –197, apr 2002.

[27] U. Lucangelo, V. Antonaglia, W. Zin, G. Berlot, L. Fontanesi, A. Peratoner, F. Bernabè, and A. Gullo, "Mechanical loads modulate tidal volume and lung washout during high-frequency percussive ventilation," *Respiratory physiology & neurobiology*, vol. 150, no. 1, pp. 44–51, 2006.

[28] F. Riscica, U. Lucangelo, M. Ferluga, and A. Accardo, "In vitro measurements of respiratory mechanics during hfpv using a mechanical lung model," *Physiological Measurement*, vol. 32, no. 6, p. 637, 2011.